

Hadronic High-energy Emission from Magnetically Arrested Disks in Radio Galaxies

SHIGEO S. KIMURA^{1,2,*} AND KENJI TOMA^{1,2}

¹Frontier Research Institute for Interdisciplinary Sciences, Tohoku University, Sendai 980-8578, Japan

²Astronomical Institute, Tohoku University, Sendai 980-8578, Japan

ABSTRACT

We propose a novel interpretation that gamma-rays from nearby radio galaxies are hadronic emission from magnetically arrested disks (MADs) around central black holes (BHs). The magnetic energy in MADs is higher than the thermal energy of the accreting plasma, where the magnetic reconnection or turbulence may efficiently accelerate non-thermal protons. They emit gamma-rays via hadronic processes, which can account for the observed gamma-rays for M87 and NGC 315. The gamma-rays efficiently produce electron-positron pairs through two-photon annihilation in the BH magnetosphere, which can screen the vacuum gap. The hadronic emission from the MADs significantly contributes to the GeV gamma-ray background and produces the multi-PeV neutrino background detectable by IceCube-Gen2.

Keywords: Radio active galactic nuclei (2134), Low-luminosity active galactic nuclei (2033), Gamma-rays (637), Accretion (14), Non-thermal radiation sources (1119), Cosmic background radiation (317)

1. INTRODUCTION

Radio galaxies are a sub-class of radio-loud active galactic nuclei (AGNs), whose jets are misaligned to the Earth. Some of them are observed from radio to GeV-TeV gamma-rays, but the emission mechanism and production site of the gamma-rays are still controversial (For a review, see Rieger & Levinson 2018). Regarding M87, a nearby radio galaxy whose jet and central region are investigated in great detail (e.g., Hada et al. 2011; Event Horizon Telescope Collaboration et al. 2019a,b,c,d,e,f), the leptonic jet models require the magnetic field of a few mG (Abdo et al. 2009; MAGIC Collaboration et al. 2020), which is much weaker than the value estimated by the radio observation (Hada et al. 2013; Kino et al. 2015). The magnetic field can be strong enough for the hadronic jet models, but they demand a jet power much higher than the estimated mass accretion power (Reynoso et al. 2011) or a high beaming factor (MAGIC Collaboration et al. 2020). The magnetosphere models in which a vacuum gap accelerates electron-positron pairs may be feasi-

ble for TeV gamma-rays, but reproducing the GeV gamma-ray data is challenging due to a hard spectrum (Levinson & Rieger 2011; Hirotani & Pu 2016; Kisaka et al. in prep.).

We propose hadronic processes in magnetically arrested disks (MADs; Narayan et al. 2003) as an alternative gamma-ray emission mechanism. Radio galaxies likely host MADs because they can efficiently launch relativistic jets (Tchekhovskoy et al. 2011; McKinney et al. 2012; Sadowski et al. 2013; Chael et al. 2019; Event Horizon Telescope Collaboration et al. 2019e; Porth et al. 2019) by the Blandford-Znajek mechanism (Blandford & Znajek 1977; Komissarov 2004; Toma & Takahara 2016). They dissipate their magnetic energies through plasma processes, such as magnetic reconnection (Ball et al. 2018a; Ripperda et al. 2020), and non-thermal particles are efficiently accelerated by reconnection (Zenitani & Hoshino 2001; Hoshino 2012; Sironi & Spitkovsky 2014; Werner et al. 2018) and/or turbulence (Lynn et al. 2014; Kimura et al. 2016; Comisso & Sironi 2018; Kimura et al. 2019b), leading to gamma-ray emission via hadronic processes (see Figure 1). Hadronic emission from the accretion flows were previously discussed as the emission mechanisms of soft gamma-rays (Mahadevan et al. 1997; Oka & Manmoto 2003; Niedźwiecki et al. 2013) and IceCube neutrinos (Kimura et al. 2015; Khiali & de Gouveia Dal Pino

Corresponding author: Shigeo S. Kimura
 shigeo@astr.tohoku.ac.jp

* JSPS Fellow

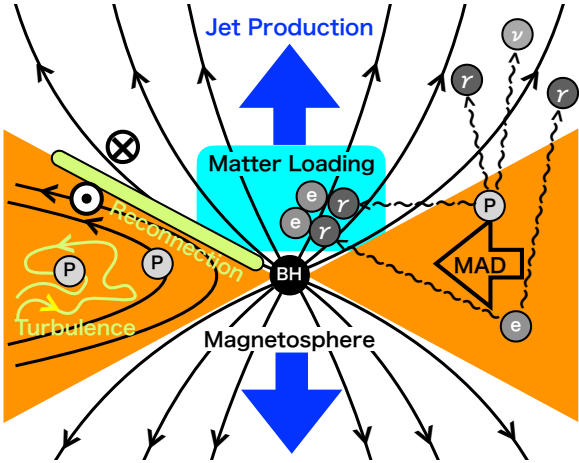


Figure 1. Schematic picture of our model. Protons are accelerated in the MAD through reconnection or turbulence, leading to hadronic gamma-ray and neutrino emissions. The gamma-rays interact with lower-energy photons emitted by thermal electrons, efficiently creating the electron-positron pairs in the magnetosphere.

2016; Kimura et al. 2019a), but has not been examined as the GeV-TeV gamma-ray emission mechanism in radio galaxies (see Rodríguez-Ramírez et al. 2019 for application to Galactic center).

In this Letter, we develop a MAD model that can reproduce gamma-ray observations for M87 and NGC 315, which are in low accretion states and detected by *Fermi*. We also estimate the contribution by MADs to the diffuse high-energy backgrounds. Furthermore, high-energy photons from MADs can create electron-positron pairs in the jet region. In previous studies, only MeV photons are considered, and the amount of those pairs for M87 is marginal to screen the gap (Levinson & Rieger 2011; Mościbrodzka et al. 2011). In our model, the GeV-TeV photons from the disk can enlarge the pair density in the jet region. We use the notation of $Q_X = Q/10^X$ in cgs unit, except for the black hole (BH) mass, M ($M_9 = M/[10^9 \text{ M}_\odot]$).

2. MAD MODEL

We calculate the photon spectra from MADs using one-zone and steady-state approximations. Our model is similar to that given in Kimura et al. (2019a), which is applicable to the hot accretion flow. We consider an accreting plasma onto a supermassive BH of mass M . The mass accretion rate, \dot{M} , and size of the plasma, R , are normalized by the Eddington rate and gravitational radius, $R = \mathcal{R}R_G = \mathcal{R}GM/c^2$ and $\dot{M}c^2 = \dot{m}L_{\text{Edd}}$ (without including the radiation efficiency factor), respectively. The hydrodynamical quantities in the MAD are analytically estimated using the

equations in Kimura et al. (2019a), which are in rough agreement with the magnetohydrodynamic (MHD) simulations (Machida & Matsumoto 2003; Narayan et al. 2012; Kimura et al. 2019b; Chael et al. 2019). Additional parameters are the viscous parameter α (Shakura & Sunyaev 1973) and the plasma beta β .

We consider emissions from thermal electrons and non-thermal protons. The spectra for the synchrotron, bremsstrahlung, and Comptonization processes by the thermal electrons are calculated by the methods given in Kimura et al. (2015). The electron temperature is determined such that the resulting photon luminosity is equal to the electron heating rate. The electron heating mechanism in hot accretion flows has yet to be established (e.g., Sironi & Narayan 2015; Zhdankin et al. 2019; Kawazura et al. 2019). We utilize the formalism by Hoshino (2018), where the ratio of heating rate for electrons to protons is given by $Q_e/Q_p \approx [(m_e T_e)/(m_p T_p)]^{1/4}$. Then, the photon luminosity by the thermal electrons is estimated to be $L_{\gamma,e} \approx (Q_e/Q_p)\epsilon_{\text{dis}}\dot{m}L_{\text{Edd}}$, where ϵ_{dis} is the energy fraction of the dissipation to accretion. We ignore the non-thermal electron component for simplicity.

The photon spectra by the thermal electrons for M87 and NGC 315 are shown in Figure 2, and the parameters and resulting quantities are tabulated in Table 1. The MAD heats up the thermal electrons to a few MeV, and they emit peaky signals in $\sim 10^{-3}$ eV by the synchrotron radiation. These photons are important targets for the photo-hadronic processes. Although the inverse Compton scattering and bremsstrahlung create higher energy photons, they are too faint to explain the observed data, and too tenuous to work as target photons.

To obtain the non-thermal proton spectrum, we solve the steady-state transport equation:

$$-\frac{d}{dE_p} \left(\frac{E_p N_{E_p}}{t_{\text{cool}}} \right) = \dot{N}_{E_p,\text{inj}} - \frac{N_{E_p}}{t_{\text{esc}}}, \quad (1)$$

where N_{E_p} is the differential proton number spectrum, t_{cool} is the cooling time, t_{esc} is the escape time, and $\dot{N}_{E_p,\text{inj}}$ is the injection terms. The analytic solution of this equation is given by

$$N_{E_p} = \frac{t_{\text{cool}}}{E_p} \int_{E_p}^{\infty} dE'_p \dot{N}_{E'_p,\text{inj}} \exp \left(- \int_{E_p}^{E'_p} \frac{t_{\text{cool}} dE_p}{t_{\text{esc}} E_p} \right). \quad (2)$$

We estimate the diffusive and infall escape timescales to be $t_{\text{diff}} \approx R^2/D_R$ and $t_{\text{fall}} \approx R/V_R$, respectively, where $D_R \approx cr_L(R/r_L)^{(q-1)}/(9\zeta)$ is the diffusion coefficient, r_L is the Larmor radius, ζ is the turbulence strength, and q is the index of the turbulence power spectrum (Kimura et al. 2015). For the proton cooling process,

Table 1. List of model parameters and physical quantities. The references for BH masses and distances are Event Horizon Telescope Collaboration et al. (2019a) for M87 and Saikia et al. (2018) for NGC 315.

Parameters of our model														
α	β	\mathcal{R}	ϵ_{dis}	η_{acc}	ζ	q	ϵ_p	s_{inj}	ϵ_j					
(M87, NGC 315)					(M87, NGC 315)									
0.3 0.1 10 0.1 10 0.5 5/3 0.05 1.5 1.0														
(6.3, 1.7) (17, 65) (0.5, 6.0)														
Physical quantities														
	B [G]	T_e [MeV]	Q_p/Q_e	$L_{\gamma,e}$ [$10^{41} \text{ erg s}^{-1}$]	$E_{p,\text{cut}}$ [eV]	L_p [$10^{42} \text{ erg s}^{-1}$]	B_h [kG]	n_{GJ} [10^{-5} cm^{-3}]	$\log(n_{\pm}/n_{\text{GJ}})$					
M87	18	2.2	12	3.4	9.7	2.0	0.31	2.8	1.44					
NGC315	121	1.2	14	9.1	5.0	6.3	2.1	71	3.33					

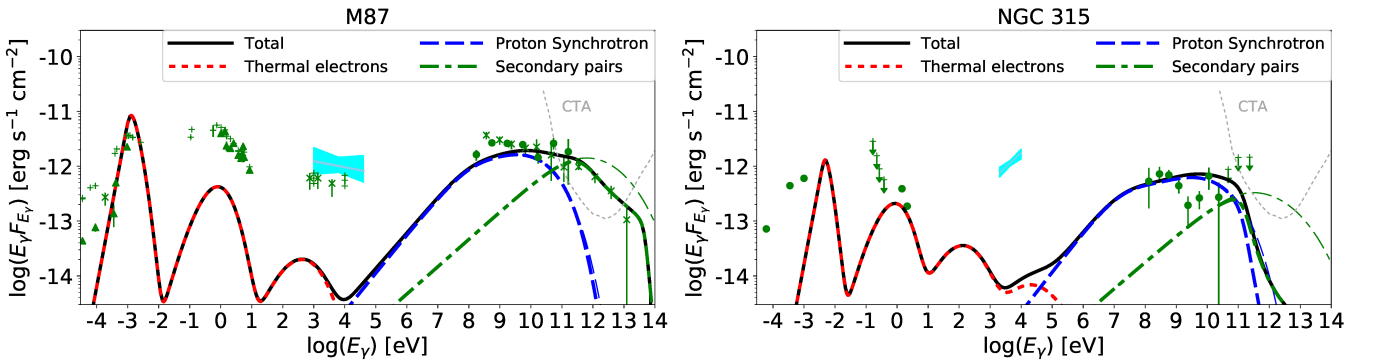


Figure 2. Broadband Spectra for M87 (left) and NGC 315 (right). The black-solid lines are total flux, blue-dashed lines are proton synchrotron, red-dotted lines are emission by thermal electrons, and green-dot-dashed lines are emission by secondary pairs produced by Bethe-Heitler process. The thick lines are the observed flux on Earth, and the thin lines are the intrinsic spectra before the attenuation. The thin-dotted lines are the sensitivity for CTA (Cherenkov Telescope Array Consortium et al. 2019). Data points are taken from MAGIC Collaboration et al. (2020); Prieto et al. (2016); Wong et al. (2017); Ait Benkhali et al. (2019) for M87 and from de Menezes et al. (2020) for NGC 315.

we take into account the pp inelastic collisions, photomeson production, Bethe-Heitler pair production, and proton synchrotron processes (see Kimura et al. 2019a). We phenomenologically write the acceleration time as $t_{\text{acc}} \approx \eta_{\text{acc}} r_L/c$, where η_{acc} is the acceleration efficiency parameter. The injection term is written as $\dot{N}_{E_p,\text{inj}} \approx \dot{N}_0 (E_p/E_{p,\text{cut}})^{-s_{\text{inj}}} \exp(-E_p/E_{p,\text{cut}})$, where s_{inj} is the injection spectral index. $E_{p,\text{cut}}$ and \dot{N}_0 are determined by $t_{\text{loss}} = t_{\text{acc}}$ and $L_p = \int \dot{N}_{E_p,\text{inj}} dE_p = \epsilon_p \dot{N}_0 c^2$, respectively, where $t_{\text{loss}}^{-1} = t_{\text{cool}}^{-1} + t_{\text{esc}}^{-1}$ is the loss timescale and ϵ_p is the cosmic-ray injection efficiency.

Figure 3 indicates the timescales as a function of E_p for M87 (left) and NGC 315 (right), whose parameters are tabulated in Table 1. For $E_p \lesssim 1$ EeV, the cooling is very inefficient, but the Bethe-Heitler and synchrotron processes are efficient for higher energies. For a higher \dot{m} , the synchrotron cooling is more efficient owing to stronger magnetic fields. MADs may accelerate the protons up to 9.7 EeV for M87 and 5.0 EeV for NGC 315,

and the particle acceleration is limited by the cooling for both cases.

We calculate the photon spectra by primary protons and secondary electron-positron pairs. For both populations, the synchrotron radiation is the dominant process, and we calculate the synchrotron spectra using the method in Finke et al. (2008), appropriately taking into account the difference between protons and electrons. To obtain the spectrum of the secondary pairs, we solve the transport equation of the pairs as in the protons. The secondary pairs are mainly produced through the Bethe-Heitler process, and the injection term of the pairs is approximated to be $E_{\pm}^2 \dot{N}_{E_{\pm},\text{inj}} \approx E_p^2 N_{E_p} t_{\text{BH}}^{-1}$, where $E_{\pm} \approx (m_e/m_p) E_p$ is the energy of the pairs (Murase et al. 2019). Other emission regions, such as inner jets and outer accretion flows, may contribute to the observed flux, so we should regard them as upper limits.

The resulting gamma-ray spectra are plotted in Figure 2 (see Table 1 for the parameter sets). For

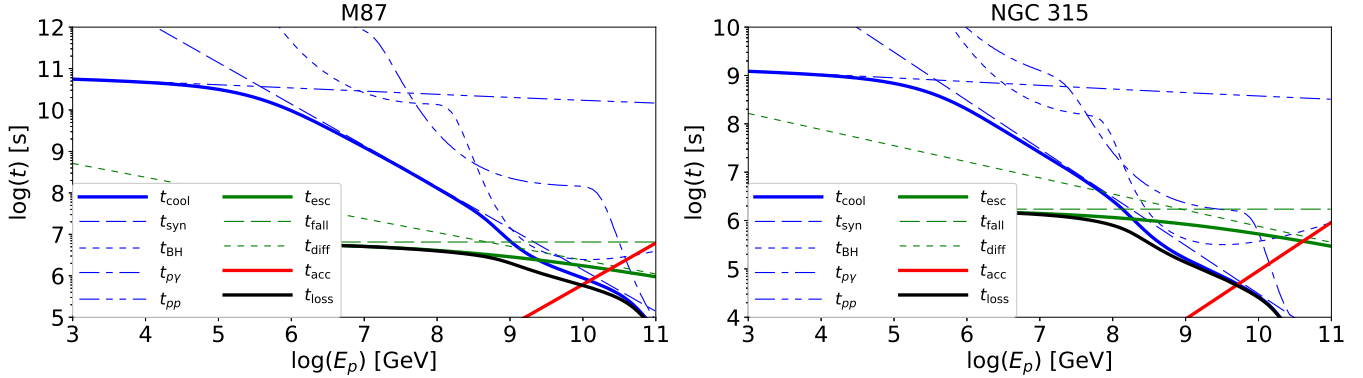


Figure 3. Cooling (blue), escape (green), loss (black), and acceleration (red) timescales as a function of the proton energy for M87 (left) and NGC 315 (right). t_{syn} , t_{BH} , $t_{p\gamma}$, and t_{pp} are the synchrotron, Bethe-Heitler, photomeson, and proton-proton cooling timescales, respectively.

M87, the proton synchrotron emission accounts for the *Fermi* data, and the secondary pairs reproduce the TeV gamma-rays for the quiescent state detected by MAGIC. TeV gamma-rays from M87 are strongly variable, and the flaring activities should be attributed to jets as they correlate with the radio and/or X-ray flares (Aharonian et al. 2006; Abramowski et al. 2012; Hada et al. 2014). For NGC 315, the proton synchrotron produces the gamma-rays in *Fermi* band, but the TeV gamma-rays by the pairs are completely absorbed, and we cannot detect them even with CTA.

3. PAIR PRODUCTION AT MAGNETOSPHERE

The polar region lacks mass supply because the centrifugal barrier and possible globally-ordered magnetic fields prevent thermal particles from entering there. The density in the region continues to decrease, leading to formation of a magnetosphere (McKinney & Gammie 2004; Nakamura et al. 2018). A vacuum gap may open in the magnetosphere when the number density is below the Goldreich-Julian density (Goldreich & Julian 1969),

$$n_{\text{GJ}} = \frac{\Omega_F B_h}{2\pi e c} \approx \frac{B_h}{8\pi e R_G} \simeq 5.6 \times 10^{-4} B_{h,3} M_9^{-1} \text{ cm}^{-3}, \quad (3)$$

where $B_h \approx \Phi_{\text{MAD}}/(2\pi R_G^2) \simeq 1.1 \times 10^3 \dot{m}_{-4}^{1/2} M_9^{-1/2}$ G is the magnetic field strength at the horizon, $\Phi_{\text{MAD}} \sim 50\sqrt{\dot{M}cR_G^2}$ is the magnetic flux for MADs (Tchekhovskoy et al. 2011), and $\Omega_F \approx c/(4R_G)$ is the angular velocity of the field lines with the efficient energy extraction (Blandford & Znajek 1977). The gap accelerates charged particles, which highly influences the structures of bulk flow and high-energy emission in the magnetosphere (see Rieger & Levinson 2018).

Here, we examine whether the gap can be screened by the gamma-rays emitted from the MAD creating

electron-positron pairs in the magnetosphere through interaction with lower energy photons. The gap could be open at $\sim 2R_G$ (Hirotani & Pu 2016; Levinson & Segev 2017; Chen & Yuan 2019; Kisaka et al. in prep.). This is smaller than the emission region of the high-energy photons, and thus, we assume the isotropic photon distribution. In the steady state, the pair production rate should be balanced by the advective escape rate, which leads to (cf. Levinson & Rieger 2011)

$$n_{\pm} \approx 2R_G \int dE_{\gamma} n_{E_{\gamma}} \int d\varepsilon_{\gamma} n_{\varepsilon_{\gamma}} \mathcal{K}(x), \quad (4)$$

where we assume the escape velocity of $c/3$, the magnetosphere size of $2R_G$, $n_{E_{\gamma}} = L_{E_{\gamma}}/(4\pi R^2 c E_{\gamma}^2)$ is the differential number density of the photons, $\mathcal{K}(x) = 0.652\sigma_T \log(x)(x^2 - 1)x^{-3}H(x - 1)$, and $x = E_{\gamma}\varepsilon_{\gamma}/(m_e^2 c^4)$ (Coppi & Blandford 1990). We find that the pair amounts are sufficient for screening the gap in M87 and NGC315 (see Table 1).

The pairs injected to the magnetosphere mainly lose their energies by emitting X-rays to MeV gamma-rays through synchrotron radiation. These photons have too low energies to further produce the pairs by themselves, but they may increase the pair production rate by acting as target photons for GeV gamma-rays. Here, we have ignored this effect to make a conservative estimate. For typical parameters of $B_h \sim 10^3$ G and $M \sim 10^9 M_{\odot}$, the Lorentz factor, γ_{\pm} , becomes ~ 1 before their advective escape. Most of the observed radio galaxies have soft photon spectra in the GeV-TeV gamma-ray band. Then, we can roughly estimate the pair density to be

$$n_{\pm} \sim \frac{\sigma_{\gamma\gamma} R_G L_{\text{GeV}} L_{\text{keV}}}{8\pi^2 R^4 c^2 E_{\text{GeV}} E_{\text{keV}}} \simeq 0.02 M_9^{-3} \mathcal{R}_1^{-4} L_{\text{GeV},41} L_{\text{keV},40} \text{ cm}^{-3}, \quad (5)$$

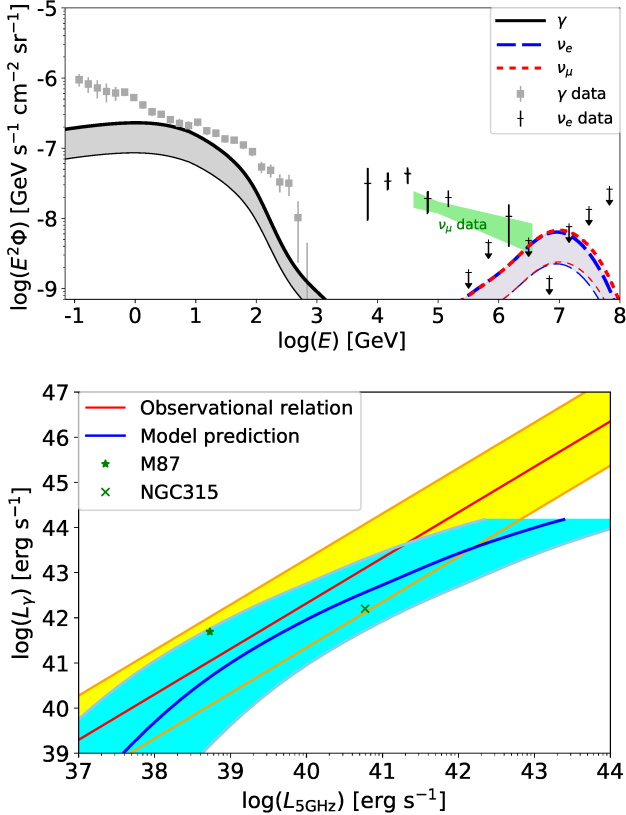


Figure 4. Top: The diffuse intensities for gamma-rays (black-solid), electron neutrinos (blue-dashed), and muon neutrinos (red-dotted). The thick and thin lines are drawn with the luminosity functions by Heckman & Best (2014) and Pracy et al. (2016), respectively. The data points are from Ackermann et al. (2015) (gamma-rays), Aartsen et al. (2020) (ν_e), and Stettner (2019) (ν_μ). Bottom: Relation of 5-GHz luminosity and gamma-ray luminosity in the LAT band. The cyan and yellow regions are our model prediction and the observed correlation by Di Mauro et al. (2014), respectively.

which is orders of magnitude higher than n_{GJ} in Equation (3).

4. DIFFUSE HIGH-ENERGY BACKGROUNDS

Radio galaxies are proposed as a source of the cosmic high-energy backgrounds of gamma-rays (Inoue 2011; Di Mauro et al. 2014; Stecker et al. 2019) and neutrinos (Becker Tjus et al. 2014; Hooper 2016). We here estimate the high-energy background intensities from MADs. The $p\gamma$ neutrino spectra are obtained using method in Kimura et al. (2017, 2018a). The neutrinos from pp interactions are negligible for the range of our interest. High-energy gamma-rays from high redshifts are attenuated through interactions with the extragalactic background light (EBL), and we use optical depth for $\gamma\gamma$

attenuation in Franceschini & Rodighiero (2017). The electromagnetic cascades initiated by EBL attenuation are negligible for the GeV gamma-ray background.

Radio galaxies are classified into two groups based on the optical line properties. One is low-excitation radio galaxies (LERGs), which have a hot accretion flow. The other is high-excitation radio galaxies (HERGs), where the optically thick disk surrounds the BH. Since our model is not applicable to HERGs, we focus on the contribution by LERGs. The local 1.4-GHz radio luminosity function of LERGs are written as $\rho_{1.4\text{GHz}} = \rho_* / [(L_{1.4\text{GHz}}/L_*)^{0.42} + (L_{1.4\text{GHz}}/L_*)^{1.66}]$, where $L_* = 1.2 \times 10^{41} \text{ erg s}^{-1}$ and $\rho_* = 4.7 \times 10^{-6} \text{ Mpc}^{-3}$ (Heckman & Best 2014). The LERG population shows little or no redshift evolution (Pracy et al. 2016), which is consistent with other low-luminosity AGN populations (Padovani et al. 2011; Ajello et al. 2014; Ueda et al. 2014). 1.4-GHz signals are attributed to the emission from the jet. We use the empirical correlation, $\log(L_{j,42}) = 0.75 \log(L_{1.4\text{GHz},40}) + 1.91$, to convert radio luminosity, $L_{1.4\text{GHz}}$, to the jet power, L_j (Cavagnolo et al. 2010). Then, we relate the jet power to the accretion rate by $L_j \sim \epsilon_j \dot{m} c^2$, where $\epsilon_j \sim 1$ is the jet production efficiency based on the simulations (Tchekhovskoy et al. 2011; Sadowski et al. 2013; Akiyama et al. 2019b) and observations (McNamara et al. 2011; Nemmen & Tchekhovskoy 2015; Turner & Shabala 2015). The radio galaxies of $M \simeq 10^9 M_\odot$ mainly contribute to the radio luminosity density (Best et al. 2005), and we fix $M = 10^9 M_\odot$ for the estimates of the diffuse intensities. Then, we convert $L_{1.4\text{GHz}}$ to \dot{m} and calculate neutrino and gamma-ray spectra for various \dot{m} to obtain the cosmic background intensities.

The resulting high-energy neutrino and gamma-ray backgrounds are shown in the top panel of Figure 4. MADs can provide a large fraction of the gamma-ray background for $E_\gamma \sim 1 - 30 \text{ GeV}$. The luminosity function has a break at $L_* \simeq 1.2 \times 10^{41} \text{ erg s}^{-1}$, and LERGs with $L_{1.4\text{GHz}} = L_*$, corresponding to $\dot{m} = \dot{m}_* \sim 0.004$, predominantly contribute to the diffuse backgrounds. Then, the gamma-ray intensity is estimated to be

$$\begin{aligned} E_\gamma^2 \Phi_\gamma &\approx \frac{c \xi_z f_{\gamma/p} f_{\text{bol}}}{4 \pi H_0} \rho_* \epsilon_p \dot{m}_* L_{\text{Edd}} \simeq 1.6 \times 10^{-7} \\ &\times M_9 \left(\frac{\epsilon_p}{0.05} \right) \left(\frac{\xi_z}{0.6} \right) \left(\frac{f_{\text{bol}} f_{\gamma/p}}{0.1} \right) \text{ GeV s}^{-1} \text{ cm}^{-2} \text{ sr}^{-1}, \end{aligned} \quad (6)$$

where ξ_z is the redshift evolution factor (Murase & Waxman 2016), f_{bol} is the bolometric correction factor, and $f_{\gamma/p} = L_\gamma / L_p$. This estimate is consistent with the observed gamma-ray background for $1 - 30 \text{ GeV}$. The cutoff energy for gamma-rays

due to the two-photon annihilation is ~ 9 GeV for LERGs of $\dot{m} \sim \dot{m}_*$, so the gamma-rays above the energy is significantly attenuated inside the source. The diffuse neutrino intensity has a peak at 10 PeV and is consistent with the extrapolation of the detected intensity (Aartsen et al. 2015; Aartsen et al. 2015). It rapidly decreases above the energy due to the pion cooling suppression. The peak intensity of the neutrinos per flavor can be estimated to be $E_\nu^2 \Phi_\nu \approx (1/3) f_{p\gamma} E_\gamma^2 \Phi_\gamma \sim 5 \times 10^{-9}$ GeV s $^{-1}$ cm $^{-2}$ sr $^{-1}$, where $f_{p\gamma} = t_{p\gamma}^{-1}/t_{\text{loss}}^{-1} \sim 0.1$ is the pion production efficiency at the peak energy. The predicted intensity is detectable by the planned experiment, IceCube-Gen2 (Aartsen et al. 2019). We should note the uncertainty of the luminosity function of LERGs. With the luminosity function given in Table 4 of Pracy et al. (2016), the diffuse intensities are a factor of 3 lower as shown by the thin lines, but the neutrinos are still detectable by IceCube-Gen2.

Observationally, the gamma-ray luminosity in the LAT band correlates with the 5-GHz luminosity (Inoue 2011; Di Mauro et al. 2014; Stecker et al. 2019). Our model can reproduce the observed correlation (the bottom panel of Figure 4), taking into account the dispersion of L_j - $L_{1.4\text{GHz}}$ relation of 0.7 dex (Cavagnolo et al. 2010). Here, we use $L_{5\text{GHz}} \approx (5/1.4)^{0.2} L_{1.4\text{GHz}}$ as in the previous works (Willott et al. 2001; Inoue 2011). For radio galaxies of $L_{5\text{GHz}} \gtrsim 10^{41}$ erg s $^{-1}$, gamma-rays from MADs are attenuated by the two-photon annihilation. Hence, our model predicts a sub-population that shows a fainter L_γ than the relation, but detecting them by LAT is challenging. For $L_{5\text{GHz}} \gtrsim 10^{43}$ erg s $^{-1}$, the assumption of the collisionless accretion flow breaks down, and jets should be responsible for the gamma-ray emission.

5. SUMMARY & DISCUSSION

We propose hadronic interactions in MADs as a novel mechanism of the gamma-ray production in radio galaxies. Non-thermal protons accelerated in MADs produce high-energy gamma-rays, which can reproduce the gamma-ray data of M87 and NGC 315. The gamma-rays from the MADs create electron-positron pairs in the magnetosphere, which may screen the gap. The MADs can be a main contributor to the extragalactic gamma-ray background for $E_\gamma \sim 1 - 30$ GeV. They also produce the extragalactic neutrino background of $E_\nu \sim 10$ PeV, which is detectable by IceCube-Gen2.

Our parameter choice of high ϵ_p and low s_{inj} is based on particle-in-cell simulations and theoretical considerations. In the relativistic reconnections with the magnetization parameter $\sigma \gtrsim 1$, most of the dissipation energy is spent to produce non-thermal

particles (Sironi & Spitkovsky 2014; Guo et al. 2016; Werner et al. 2018; Petropoulou & Sironi 2018). Recent general relativistic MHD (GRMHD) simulations revealed that the accreting plasma may have current sheets with $\sigma \gtrsim 1$ (Ball et al. 2018a; Ripperda et al. 2020), suggesting a high value of ϵ_p in the MADs. Nevertheless, $\epsilon_p \lesssim \epsilon_{\text{dis}}$ should be satisfied, otherwise the accretion flow becomes the standard thin disk due to the efficient cooling by the hadronic processes (Kimura et al. 2014). The non-thermal particles are further accelerated by the stochastic acceleration process by large-scale turbulence, which may lead to a harder spectral index of $s_{\text{inj}} < 2$ (Becker et al. 2006; Stawarz & Petrosian 2008).

In the strongly magnetized plasma, non-thermal electrons are also expected to be accelerated by the magnetic reconnection (Sironi & Spitkovsky 2014; Werner et al. 2018; Ball et al. 2018b). They emit X-rays and MeV gamma-rays by synchrotron radiation. If the non-thermal electron are produced as efficiently as protons, the X-rays may overshoot the observed data. Also, the X-ray and MeV gamma-rays can attenuate the GeV-TeV photons and initiate electromagnetic cascades. On the other hand, for the case with a much lower electron acceleration efficiency as expected in Fermi-type acceleration, non-thermal electrons are negligible.

Radio galaxies are also discussed as the origin of the ultrahigh-energy cosmic-rays (e.g. Takahara 1990; Murase et al. 2012; Rodrigues et al. 2018; Eichmann et al. 2018). Although MADs can accelerate the protons up to $\sim 1 - 10$ EeV, they mainly lose their energies by hadronic processes. Also, the accelerated particles in MADs are likely to be the same composition as the accreting plasma of the solar abundance, which is inconsistent with the Auger data that support a heavier composition (Aab et al. 2014). Thus, majority of the observed UHECRs should be accelerated in another cite (e.g., Caprioli 2015; Kimura et al. 2018b). For $\dot{m} \lesssim 10^{-4}$, non-negligible fraction of protons can escape from the system, and may be observed on Earth. Takami et al. (2016) estimated the upper limit of the UHECR luminosity to be $\sim 10^{42}$ erg s $^{-1}$ for the object of $d_L \sim 40$ Mpc using the isotropic arrival direction of UHECRs. The UHECR luminosity of M87 in our model is lower, but the distance is closer. It remains as a future work to investigate the possibility whether MADs in nearby radio galaxies contribute to the observed CRs for 1-10 EeV.

ACKNOWLEDGMENTS

We thank Shota Kisaka for discussion and Daniel Mazin for comments in the workshop "Active Galactic Nucleus Jets in the Event Horizon Telescope Era" at Tohoku University on Jan 20-22, 2020. This work is partly supported by JSPS Research Fellowship No. 19J00198 (S.S.K.) and KAKENHI No. 18H01245 (K.T.).

REFERENCES

- Aab, A., Abreu, P., Aglietta, M., et al. 2014, *PhRvD*, 90, 122005, doi: [10.1103/PhysRevD.90.122005](https://doi.org/10.1103/PhysRevD.90.122005)
- Aartsen, M. G., Abraham, K., Ackermann, M., et al. 2015, *ApJ*, 809, 98, doi: [10.1088/0004-637X/809/1/98](https://doi.org/10.1088/0004-637X/809/1/98)
- Aartsen, M. G., et al. 2015, *Phys. Rev. Lett.*, 115, 081102, doi: [10.1103/PhysRevLett.115.081102](https://doi.org/10.1103/PhysRevLett.115.081102)
- . 2019. <https://arxiv.org/abs/1911.02561>
- . 2020. <https://arxiv.org/abs/2001.09520>
- Abdo, A. A., Ackermann, M., Ajello, M., et al. 2009, *ApJ*, 707, 55, doi: [10.1088/0004-637X/707/1/55](https://doi.org/10.1088/0004-637X/707/1/55)
- Abramowski, A., Acero, F., Aharonian, F., et al. 2012, *ApJ*, 746, 151, doi: [10.1088/0004-637X/746/2/151](https://doi.org/10.1088/0004-637X/746/2/151)
- Ackermann, M., et al. 2015, *Astrophys. J.*, 799, 86, doi: [10.1088/0004-637X/799/1/86](https://doi.org/10.1088/0004-637X/799/1/86)
- Aharonian, F., Akhperjanian, A. G., Bazer-Bachi, A. R., et al. 2006, *Science*, 314, 1424, doi: [10.1126/science.1134408](https://doi.org/10.1126/science.1134408)
- Ait Benkhali, F., Chakraborty, N., & Rieger, F. M. 2019, *A&A*, 623, A2, doi: [10.1051/0004-6361/201732334](https://doi.org/10.1051/0004-6361/201732334)
- Ajello, M., Romani, R. W., Gasparrini, D., et al. 2014, *ApJ*, 780, 73, doi: [10.1088/0004-637X/780/1/73](https://doi.org/10.1088/0004-637X/780/1/73)
- Akiyama, K., et al. 2019a, *Astrophys. J.*, 875, L1, doi: [10.3847/2041-8213/ab0ec7](https://doi.org/10.3847/2041-8213/ab0ec7)
- . 2019b, *Astrophys. J.*, 875, L5, doi: [10.3847/2041-8213/ab0f43](https://doi.org/10.3847/2041-8213/ab0f43)
- Ball, D., Özel, F., Psaltis, D., Chan, C.-K., & Sironi, L. 2018a, *ApJ*, 853, 184, doi: [10.3847/1538-4357/aaa42f](https://doi.org/10.3847/1538-4357/aaa42f)
- Ball, D., Sironi, L., & Özel, F. 2018b, *ApJ*, 862, 80, doi: [10.3847/1538-4357/aac820](https://doi.org/10.3847/1538-4357/aac820)
- Becker, P. A., Le, T., & Dermer, C. D. 2006, *ApJ*, 647, 539, doi: [10.1086/505319](https://doi.org/10.1086/505319)
- Becker Tjus, J., Eichmann, B., Halzen, F., Kheirandish, A., & Saba, S. M. 2014, *PhRvD*, 89, 123005, doi: [10.1103/PhysRevD.89.123005](https://doi.org/10.1103/PhysRevD.89.123005)
- Best, P. N., Kauffmann, G., Heckman, T. M., et al. 2005, *MNRAS*, 362, 25, doi: [10.1111/j.1365-2966.2005.09192.x](https://doi.org/10.1111/j.1365-2966.2005.09192.x)
- Blandford, R. D., & Znajek, R. L. 1977, *MNRAS*, 179, 433, doi: [10.1093/mnras/179.3.433](https://doi.org/10.1093/mnras/179.3.433)
- Caprioli, D. 2015, *ApJL*, 811, L38, doi: [10.1088/2041-8205/811/2/L38](https://doi.org/10.1088/2041-8205/811/2/L38)
- Cavagnolo, K. W., McNamara, B. R., Nulsen, P. E. J., et al. 2010, *ApJ*, 720, 1066, doi: [10.1088/0004-637X/720/2/1066](https://doi.org/10.1088/0004-637X/720/2/1066)
- Chael, A., Narayan, R., & Johnson, M. D. 2019, *MNRAS*, 486, 2873, doi: [10.1093/mnras/stz988](https://doi.org/10.1093/mnras/stz988)
- Chen, A. Y., & Yuan, Y. 2019, arXiv e-prints, arXiv:1908.06919. <https://arxiv.org/abs/1908.06919>
- Cherenkov Telescope Array Consortium, Acharya, B. S., Agudo, I., et al. 2019, *Science with the Cherenkov Telescope Array*, doi: [10.1142/10986](https://doi.org/10.1142/10986)
- Comisso, L., & Sironi, L. 2018, *PhRvL*, 121, 255101, doi: [10.1103/PhysRevLett.121.255101](https://doi.org/10.1103/PhysRevLett.121.255101)
- Coppi, P. S., & Blandford, R. D. 1990, *MNRAS*, 245, 453
- de Menezes, R., Nemmen, R., Finke, J. D., Almeida, I., & Rani, B. 2020, *MNRAS*, 492, 4120, doi: [10.1093/mnras/staa083](https://doi.org/10.1093/mnras/staa083)
- Di Mauro, M., Calore, F., Donato, F., Ajello, M., & Latronico, L. 2014, *ApJ*, 780, 161, doi: [10.1088/0004-637X/780/2/161](https://doi.org/10.1088/0004-637X/780/2/161)
- Eichmann, B., Rachen, J. P., Merten, L., van Vliet, A., & Becker Tjus, J. 2018, *JCAP*, 2018, 036, doi: [10.1088/1475-7516/2018/02/036](https://doi.org/10.1088/1475-7516/2018/02/036)
- Event Horizon Telescope Collaboration, Akiyama, K., Alberdi, A., et al. 2019a, *ApJL*, 875, L1, doi: [10.3847/2041-8213/ab0ec7](https://doi.org/10.3847/2041-8213/ab0ec7)
- . 2019b, *ApJL*, 875, L2, doi: [10.3847/2041-8213/ab0c96](https://doi.org/10.3847/2041-8213/ab0c96)
- . 2019c, *ApJL*, 875, L3, doi: [10.3847/2041-8213/ab0c57](https://doi.org/10.3847/2041-8213/ab0c57)
- . 2019d, *ApJL*, 875, L4, doi: [10.3847/2041-8213/ab0e85](https://doi.org/10.3847/2041-8213/ab0e85)
- . 2019e, *ApJL*, 875, L5, doi: [10.3847/2041-8213/ab0f43](https://doi.org/10.3847/2041-8213/ab0f43)
- . 2019f, *ApJL*, 875, L6, doi: [10.3847/2041-8213/ab1141](https://doi.org/10.3847/2041-8213/ab1141)
- Finke, J. D., Dermer, C. D., & Böttcher, M. 2008, *ApJ*, 686, 181, doi: [10.1086/590900](https://doi.org/10.1086/590900)
- Franceschini, A., & Rodighiero, G. 2017, *A&A*, 603, A34, doi: [10.1051/0004-6361/201629684](https://doi.org/10.1051/0004-6361/201629684)
- Goldreich, P., & Julian, W. H. 1969, *ApJ*, 157, 869, doi: [10.1086/150119](https://doi.org/10.1086/150119)

- Guo, F., Li, X., Li, H., et al. 2016, ApJL, 818, L9, doi: [10.3847/2041-8205/818/1/L9](https://doi.org/10.3847/2041-8205/818/1/L9)
- Hada, K., Doi, A., Kino, M., et al. 2011, Nature, 477, 185, doi: [10.1038/nature10387](https://doi.org/10.1038/nature10387)
- Hada, K., Kino, M., Doi, A., et al. 2013, ApJ, 775, 70, doi: [10.1088/0004-637X/775/1/70](https://doi.org/10.1088/0004-637X/775/1/70)
- Hada, K., Giroletti, M., Kino, M., et al. 2014, ApJ, 788, 165, doi: [10.1088/0004-637X/788/2/165](https://doi.org/10.1088/0004-637X/788/2/165)
- Heckman, T. M., & Best, P. N. 2014, ARA&A, 52, 589, doi: [10.1146/annurev-astro-081913-035722](https://doi.org/10.1146/annurev-astro-081913-035722)
- Hirotani, K., & Pu, H.-Y. 2016, ApJ, 818, 50, doi: [10.3847/0004-637X/818/1/50](https://doi.org/10.3847/0004-637X/818/1/50)
- Hooper, D. 2016, Journal of Cosmology and Astro-Particle Physics, 2016, 002, doi: [10.1088/1475-7516/2016/09/002](https://doi.org/10.1088/1475-7516/2016/09/002)
- Hoshino, M. 2012, Physical Review Letters, 108, 135003, doi: [10.1103/PhysRevLett.108.135003](https://doi.org/10.1103/PhysRevLett.108.135003)
- . 2018, ApJL, 868, L18, doi: [10.3847/2041-8213/aaef3a](https://doi.org/10.3847/2041-8213/aaef3a)
- Inoue, Y. 2011, ApJ, 733, 66, doi: [10.1088/0004-637X/733/1/66](https://doi.org/10.1088/0004-637X/733/1/66)
- Kawazura, Y., Barnes, M., & Schekochihin, A. A. 2019, Proceedings of the National Academy of Science, 116, 771, doi: [10.1073/pnas.1812491116](https://doi.org/10.1073/pnas.1812491116)
- Khiali, B., & de Gouveia Dal Pino, E. M. 2016, MNRAS, 455, 838, doi: [10.1093/mnras/stv2337](https://doi.org/10.1093/mnras/stv2337)
- Kimura, S. S., Murase, K., Bartos, I., et al. 2018a, PhRvD, 98, 043020, doi: [10.1103/PhysRevD.98.043020](https://doi.org/10.1103/PhysRevD.98.043020)
- Kimura, S. S., Murase, K., & Mészáros, P. 2019a, PhRvD, 100, 083014, doi: [10.1103/PhysRevD.100.083014](https://doi.org/10.1103/PhysRevD.100.083014)
- Kimura, S. S., Murase, K., Mészáros, P., & Kiuchi, K. 2017, ApJL, 848, L4, doi: [10.3847/2041-8213/aa8d14](https://doi.org/10.3847/2041-8213/aa8d14)
- Kimura, S. S., Murase, K., & Toma, K. 2015, ApJ, 806, 159, doi: [10.1088/0004-637X/806/2/159](https://doi.org/10.1088/0004-637X/806/2/159)
- Kimura, S. S., Murase, K., & Zhang, B. T. 2018b, PhRvD, 97, 023026, doi: [10.1103/PhysRevD.97.023026](https://doi.org/10.1103/PhysRevD.97.023026)
- Kimura, S. S., Toma, K., Suzuki, T. K., & Inutsuka, S.-i. 2016, ApJ, 822, 88, doi: [10.3847/0004-637X/822/2/88](https://doi.org/10.3847/0004-637X/822/2/88)
- Kimura, S. S., Toma, K., & Takahara, F. 2014, ApJ, 791, 100, doi: [10.1088/0004-637X/791/2/100](https://doi.org/10.1088/0004-637X/791/2/100)
- Kimura, S. S., Tomida, K., & Murase, K. 2019b, MNRAS, 485, 163, doi: [10.1093/mnras/stz329](https://doi.org/10.1093/mnras/stz329)
- Kino, M., Takahara, F., Hada, K., et al. 2015, ApJ, 803, 30, doi: [10.1088/0004-637X/803/1/30](https://doi.org/10.1088/0004-637X/803/1/30)
- Komissarov, S. S. 2004, MNRAS, 350, 427, doi: [10.1111/j.1365-2966.2004.07598.x](https://doi.org/10.1111/j.1365-2966.2004.07598.x)
- Levinson, A., & Rieger, F. 2011, ApJ, 730, 123, doi: [10.1088/0004-637X/730/2/123](https://doi.org/10.1088/0004-637X/730/2/123)
- Levinson, A., & Segev, N. 2017, PhRvD, 96, 123006, doi: [10.1103/PhysRevD.96.123006](https://doi.org/10.1103/PhysRevD.96.123006)
- Lynn, J. W., Quataert, E., Chandran, B. D. G., & Parrish, I. J. 2014, ApJ, 791, 71, doi: [10.1088/0004-637X/791/1/71](https://doi.org/10.1088/0004-637X/791/1/71)
- Machida, M., & Matsumoto, R. 2003, ApJ, 585, 429, doi: [10.1086/346070](https://doi.org/10.1086/346070)
- MAGIC Collaboration, Acciari, V. A., Ansoldi, S., et al. 2020, MNRAS, 492, 5354, doi: [10.1093/mnras/staa014](https://doi.org/10.1093/mnras/staa014)
- Mahadevan, R., Narayan, R., & Krolik, J. 1997, ApJ, 486, 268
- McKinney, J. C., & Gammie, C. F. 2004, ApJ, 611, 977, doi: [10.1086/422244](https://doi.org/10.1086/422244)
- McKinney, J. C., Tchekhovskoy, A., & Blandford, R. D. 2012, MNRAS, 423, 3083, doi: [10.1111/j.1365-2966.2012.21074.x](https://doi.org/10.1111/j.1365-2966.2012.21074.x)
- McNamara, B. R., Rohanizadegan, M., & Nulsen, P. E. J. 2011, ApJ, 727, 39, doi: [10.1088/0004-637X/727/1/39](https://doi.org/10.1088/0004-637X/727/1/39)
- Mościbrodzka, M., Gammie, C. F., Dolence, J. C., & Shiokawa, H. 2011, ApJ, 735, 9, doi: [10.1088/0004-637X/735/1/9](https://doi.org/10.1088/0004-637X/735/1/9)
- Murase, K., Dermer, C. D., Takami, H., & Migliori, G. 2012, Astrophys. J., 749, 63, doi: [10.1088/0004-637X/749/1/63](https://doi.org/10.1088/0004-637X/749/1/63)
- Murase, K., Kimura, S. S., & Meszaros, P. 2019, arXiv e-prints, arXiv:1904.04226, <https://arxiv.org/abs/1904.04226>
- Murase, K., & Waxman, E. 2016, Phys. Rev., D94, 103006, doi: [10.1103/PhysRevD.94.103006](https://doi.org/10.1103/PhysRevD.94.103006)
- Nakamura, M., Asada, K., Hada, K., et al. 2018, ApJ, 868, 146, doi: [10.3847/1538-4357/aaeb2d](https://doi.org/10.3847/1538-4357/aaeb2d)
- Narayan, R., Igumenshchev, I. V., & Abramowicz, M. A. 2003, PASJ, 55, L69, doi: [10.1093/pasj/55.6.L69](https://doi.org/10.1093/pasj/55.6.L69)
- Narayan, R., SÄ dowski, A., Penna, R. F., & Kulkarni, A. K. 2012, MNRAS, 426, 3241, doi: [10.1111/j.1365-2966.2012.22002.x](https://doi.org/10.1111/j.1365-2966.2012.22002.x)
- Nemmen, R. S., & Tchekhovskoy, A. 2015, MNRAS, 449, 316, doi: [10.1093/mnras/stv260](https://doi.org/10.1093/mnras/stv260)
- Niedźwiecki, A., Xie, F.-G., & Stepnik, A. 2013, MNRAS, 432, 1576, doi: [10.1093/mnras/stt573](https://doi.org/10.1093/mnras/stt573)
- Oka, K., & Manmoto, T. 2003, MNRAS, 340, 543, doi: [10.1046/j.1365-8711.2003.06476.x](https://doi.org/10.1046/j.1365-8711.2003.06476.x)
- Padovani, P., Miller, N., Kellermann, K. I., et al. 2011, ApJ, 740, 20, doi: [10.1088/0004-637X/740/1/20](https://doi.org/10.1088/0004-637X/740/1/20)
- Petropoulou, M., & Sironi, L. 2018, MNRAS, 481, 5687, doi: [10.1093/mnras/sty2702](https://doi.org/10.1093/mnras/sty2702)
- Porth, O., Chatterjee, K., Narayan, R., et al. 2019, ApJS, 243, 26, doi: [10.3847/1538-4365/ab29fd](https://doi.org/10.3847/1538-4365/ab29fd)
- Pracy, M. B., Ching, J. H. Y., Sadler, E. M., et al. 2016, MNRAS, 460, 2, doi: [10.1093/mnras/stw910](https://doi.org/10.1093/mnras/stw910)

- Prieto, M. A., Fernández-Ontiveros, J. A., Markoff, S., Espada, D., & González-Martín, O. 2016, MNRAS, 457, 3801, doi: [10.1093/mnras/stw166](https://doi.org/10.1093/mnras/stw166)
- Reynoso, M. M., Medina, M. C., & Romero, G. E. 2011, A&A, 531, A30, doi: [10.1051/0004-6361/201014998](https://doi.org/10.1051/0004-6361/201014998)
- Rieger, F., & Levinson, A. 2018, Galaxies, 6, 116, doi: [10.3390/galaxies6040116](https://doi.org/10.3390/galaxies6040116)
- Ripperda, B., Bacchini, F., & Philippov, A. 2020, arXiv e-prints, arXiv:2003.04330. <https://arxiv.org/abs/2003.04330>
- Rodrigues, X., Fedynitch, A., Gao, S., Boncioli, D., & Winter, W. 2018, ApJ, 854, 54, doi: [10.3847/1538-4357/aaa7ee](https://doi.org/10.3847/1538-4357/aaa7ee)
- Rodríguez-Ramírez, J. C., de Gouveia Dal Pino, E. M., & Alves Batista, R. 2019, ApJ, 879, 6, doi: [10.3847/1538-4357/ab212e](https://doi.org/10.3847/1538-4357/ab212e)
- Saikia, P., Körding, E., Coppejans, D. L., et al. 2018, A&A, 616, A152, doi: [10.1051/0004-6361/201833233](https://doi.org/10.1051/0004-6361/201833233)
- Sądowski, A., Narayan, R., Penna, R., & Zhu, Y. 2013, MNRAS, 436, 3856, doi: [10.1093/mnras/stt1881](https://doi.org/10.1093/mnras/stt1881)
- Shakura, N. I., & Sunyaev, R. A. 1973, A&A, 24, 337
- Sironi, L., & Narayan, R. 2015, ApJ, 800, 88, doi: [10.1088/0004-637X/800/2/88](https://doi.org/10.1088/0004-637X/800/2/88)
- Sironi, L., & Spitkovsky, A. 2014, ApJ, 783, L21, doi: [10.1088/2041-8205/783/1/L21](https://doi.org/10.1088/2041-8205/783/1/L21)
- Stawarz, Ł., & Petrosian, V. 2008, ApJ, 681, 1725, doi: [10.1086/588813](https://doi.org/10.1086/588813)
- Stecker, F. W., Shrader, C. R., & Malkan, M. A. 2019, ApJ, 879, 68, doi: [10.3847/1538-4357/ab23ee](https://doi.org/10.3847/1538-4357/ab23ee)
- Stettner, J. 2019, in International Cosmic Ray Conference, Vol. 36, 36th International Cosmic Ray Conference (ICRC2019), 1017. <https://arxiv.org/abs/1908.09551>
- Takahara, F. 1990, Progress of Theoretical Physics, 83, 1071, doi: [10.1143/PTP.83.1071](https://doi.org/10.1143/PTP.83.1071)
- Takami, H., Murase, K., & Dermer, C. D. 2016, ApJ, 817, 59, doi: [10.3847/0004-637X/817/1/59](https://doi.org/10.3847/0004-637X/817/1/59)
- Tchekhovskoy, A., Narayan, R., & McKinney, J. C. 2011, MNRAS, 418, L79, doi: [10.1111/j.1745-3933.2011.01147.x](https://doi.org/10.1111/j.1745-3933.2011.01147.x)
- Toma, K., & Takahara, F. 2016, Progress of Theoretical and Experimental Physics, 2016, 063E01, doi: [10.1093/ptep/ptw081](https://doi.org/10.1093/ptep/ptw081)
- Turner, R. J., & Shabala, S. S. 2015, ApJ, 806, 59, doi: [10.1088/0004-637X/806/1/59](https://doi.org/10.1088/0004-637X/806/1/59)
- Ueda, Y., Akiyama, M., Hasinger, G., Miyaji, T., & Watson, M. G. 2014, ApJ, 786, 104, doi: [10.1088/0004-637X/786/2/104](https://doi.org/10.1088/0004-637X/786/2/104)
- Werner, G. R., Uzdensky, D. A., Begelman, M. C., Cerutti, B., & Nalewajko, K. 2018, MNRAS, 473, 4840, doi: [10.1093/mnras/stx2530](https://doi.org/10.1093/mnras/stx2530)
- Willott, C. J., Rawlings, S., Blundell, K. M., Lacy, M., & Eales, S. A. 2001, MNRAS, 322, 536, doi: [10.1046/j.1365-8711.2001.04101.x](https://doi.org/10.1046/j.1365-8711.2001.04101.x)
- Wong, K.-W., Nemmen, R. S., Irwin, J. A., & Lin, D. 2017, ApJL, 849, L17, doi: [10.3847/2041-8213/aa92c2](https://doi.org/10.3847/2041-8213/aa92c2)
- Zenitani, S., & Hoshino, M. 2001, ApJ, 562, L63, doi: [10.1086/337972](https://doi.org/10.1086/337972)
- Zhdankin, V., Uzdensky, D. A., Werner, G. R., & Begelman, M. C. 2019, PhRvL, 122, 055101, doi: [10.1103/PhysRevLett.122.055101](https://doi.org/10.1103/PhysRevLett.122.055101)